Growth of face-centred-cubic titanium on aluminium

S K Kim, F Jona and P M Marcus

Department of Materials Science and Engineering, State University of New York, Stony Brook, NY 11794-2275, USA

Abstract. Ultrathin films of Ti are grown on Al{001} and Al{110} substrates and studied by quantitative low-energy electron diffraction (QLEED). On Al{001}, high-coverage films (thicker than about 10 Å) exhibit a well-developed 1×1 phase. QLEED finds the bulk of a 25 Å film to have a body-centred tetragonal structure with $a = 2.864$ Å and $c = 4.28$ Å. Strain analysis shows that this structure cannot be strained body-centred cubic and identifies the equilibrium (i.e., the unstrained) phase of the film grown as face-centred cubic (fcc). This result is a direct proof of the existence of an epitaxially stabilized fcc modification of Ti (which is not encountered in nature at any temperature), whose lattice constant is found to be 4.15 Å. On Al{110}, the films are found to grow to a thickness of only 5 to 6 Å, after which the LEED pattern is almost obliterated. A 2 Å film is shown to be a pseudomorphic overlayer at a distance of 1.58 Å from the substrate. On Al{001}, low-coverage Ti films exhibit a weak $c(2 \times 2)$ LEED pattern, but the associated surface structure could not be determined; partial results indicate that the Ti atoms may reside in the second layer of the substrate.

1. Introduction

A recent paper by Saleh, Shutthanandan and Smith [1] (SSS) reports the growth of ultrathin metastable Ti films with a face-centred-cubic (fcc) structure on Al{110} surfaces. The films were reportedly grown to a thickness of five atomic layers, after which 'an undetermined combination of island formation and Ti–Al interdiffusion' was found to occur.

The stable phase of Ti at room temperature (α-Ti) is hexagonal close-packed (hcp) with [2] $a = 2.9511$ Å and $c = 4.6843$ Å. A transition to β-Ti, with body-centred-cubic (bcc) structure, occurs at 882 °C: Pearson [2] lists the lattice constant as $a_0 = 3.3065$ Å at 900 °C. Thus, an fcc phase of Ti is not encountered in nature at any temperature. A value for the lattice constant of fcc Ti is available from the first-principles band-structure calculations of Moruzzi and Marcus [3] as $a_0 = 4.08$ Å. Since the lattice constant of Al is $a_0 = 4.0496$ Å the (theoretical) misfit between fcc Ti and fcc Al is only -0.75%, which makes the pseudomorphic growth of an epitaxially stabilized strained fcc phase of Ti on Al favourable.

The argument presented by SSS [1] for fcc structure of the Ti films grown on Al{110} is good, but indirect, and is not a quantitative structure determination. It is based on the one hand upon shadowing of the Al atoms on the substrate surface by Ti atoms, as revealed by high-energy ion scattering (HEIS), and on the other hand upon the observation of 1×1 low-energy electron diffraction (LEED) patterns for coverages of the substrate surface by Ti of up to about five atomic layers (no intensity spectra were recorded). The structure assignment was supported by the exclusion, for a number of different reasons, of other

possible candidates for the structure of the pseudomorphic film, namely, bcc Ti, hcp Ti, a TiAl alloy, or/and Ti hydrides [1].

The possible existence of a new crystallographic modification of Ti is sufficiently interesting, we believe, to justify another look at the problem with the purpose of finding direct quantitative evidence for the fcc structure. Such evidence can be provided by a determination of the atomic structure of the Ti films by quantitative low-energy electron diffraction (QLEED). QLEED analysis can determine the atomic structure, including relaxed positions in the surface layers and the bulk layer spacing. A strain analysis requires knowledge of the elastic constants of the new phase fcc Ti, which are unknown, but fortunately a reasonable estimate can be made from first-principles theory.

We report here the results of a study of the epitaxial growth of Ti on Al{110} and on Al{001}. The experimental tools used in this study are Auger electron spectroscopy (AES) for the analysis of the chemical state of the substrate surface, and QLEED for the structure analysis of the films. Basically, the experiments confirm the findings of SSS, albeit with some quantitative differences to be discussed later. However, convincing evidence for the existence of epitaxially stabilized fcc Ti was not found in the experiments with Al{110}, but was found in the experiments with Al{001}. Strain analysis, combined with an estimate of the elastic constants of fcc Ti, permits us to exclude strained bcc Ti and yields a reasonable estimate of the equilibrium lattice constant of fcc Ti.

2. Experiments

All of the experiments were done in a vacuum chamber at a base pressure of about 1×10^{-10} Torr (except during ion bombardments) featuring front-view LEED optics and a separate electron gun for AES scans with the LEED optics in the retarding-field analyser mode.

The aluminium substrates were platelets oriented on the nominal plane {110} or {001} within $0.5°$. It must be stated, however, that the surface quality was different in the two cases. The Al{001} surface was very flat and mirror-like, whereas the Al{110} surface was visibly rougher, as is evident from energy-dependent widths of the diffracted beams in the LEED pattern. We do not know whether this difference in morphology is responsible for the differences in the experimental results described below, but we wish to record the observation for possible future reference.

The titanium source was a Ti wire with 0.030 inch (0.76 mm) diameter heated by passage of an electric current to provide deposition rates varying from 0.2 Å min^{-1} (for the thinnest films grown) to 1 Å min^{-1} (for the thickest films grown). The surface coverage was estimated from the ratio of the Ti AES line at 27 eV (I_{Ti}^{27}) to the Al AES line at 68 eV (I_{Al}^{68}) using the formula

$$R = \frac{I_{Ti}^{27}}{I_{Al}^{68}} = R_0 \frac{1 - \exp(-d/\lambda_{Ti}^{27})}{\exp(-d/\lambda_{Al}^{68})} \tag{1}$$

where $R_0 = I_{Ti}^{\infty}/I_{Al}^{\infty}$ is the ratio of the corresponding AES lines from very thick samples (data from [4]), the λs are the inelastic mean free paths and d is the thickness of a Ti film *assumed* to be uniformly flat. The inelastic mean free paths were taken from [5]: $\lambda_{Ti}^{27} = 4.03$ Å, $\lambda_{Al}^{68} = 4.00$ Å. It is clear that the d-values determined with equation (1) yield only the thicknesses of layer equivalents, i.e., of uniform films that would produce the same AES signals as observed experimentally. In any case, surface coverages determined in this way may be in error by as much as $\pm 50\%$, primarily because of uncertainties in the values of the inelastic mean free paths.

The experimental procedures were typically as follows. The substrate surface was cleaned by sequences of argon-ion bombardments (2×10^{-5} Torr of Ar gas, 375 V, 1 μA) and anneals (400 to 450 °C for 3 to 4 h). Surface cleanness and crystallinity were checked with AES and LEED, respectively. Titanium was deposited on the clean surface (which was neither heated nor cooled) very slowly at first: after each deposition, lasting typically about 5 to 10 min, the surface was checked again by both AES and LEED. When appropriate, LEED intensities were measured for several beams with a video-LEED system described elsewhere [6]. Eventually, the surface was cleaned again by Ar-ion bombardments and the growth process repeated.

3. Observations

The evolution of a LEED pattern in the very early stages of deposition of foreign atoms on a clean surface can sometimes provide information about the growth mode [7], especially if the chemistry on the surface is known from concomitant AES experiments.

In general, the increase in the background of the LEED pattern and broadening of the diffraction spots are due to the presence of disordered steps and defects, and are therefore indicative of island growth. If the diffracted intensities or, more precisely, the intensities versus voltage curves, the so-called $I(V)$-spectra, are the same as those from the clean substrate surface, then we can conclude that the islands are sufficiently small that they do not contribute to the coherent LEED signal, i.e., only the bare areas of the substrate surface contribute. If the $I(V)$-curves do change, and the background increases markedly, then the islands are probably large enough to contribute to the signal. In this case, QLEED is not likely to be successful in describing the growth because the number of atomic layers in each island is not known and neither is the number of islands: thus, the $I(V)$-curves result from unknown contribution from unknown numbers of multilayer islands and bare substrate areas. Only when the $I(V)$-curves change with surface coverage *and* the background remains low can we say with reasonable confidence that the growth is probably layer-by-layer. In this case, QLEED may be able to give quantitative information about the crystallography of successive layers during growth (see [7] and references cited therein).

In the present study, the LEED pattern exhibits a notable increase of the background and broadening of the diffracted beams, and the $I(V)$-spectra do change with increasing coverage with respect to those from the clean surface; hence the growth of Ti on either Al{110} or Al{001} very probably occurs by way of island formation. But the behaviour is different on the two surfaces. On Al{110} the LEED pattern worsens irreversibly with increasing surface coverage: at coverages of about 5 to 6 Å all but two diffracted beams have disappeared in the high background (the exceptions are the 10 and the 01 beams, which are still detectable, but at electron energies between 40 and 50 eV only).

On Al{001}, the background also increases in the early stages, and the $I(V)$-curves change—in fact, c(2×2) develops, albeit with fairly broad fractional-order beams. However, beyond Ti coverages of about 10 Å the background decreases, the pattern is again 1×1 (i.e., the fractional-order beams vanish) and remains fairly sharp up to coverages of about 25 Å. At this coverage, the largest coverage attained in this study, the Al signal in the AES scans is barely detectable above the noise, thus allowing us to reach the conclusion that the film, although certainly not very flat, consists almost exclusively of Ti. That the film is pseudomorphic with the substrate is evident from the fact that the geometry of the LEED pattern is identical to that of the clean Al{001} substrate, i.e., the in-plane lattice constant of the Ti film is equal to that of Al{001}.

We may conclude that: (1) the growth of Ti on Al{110} and Al{001} is not layer-by-

layer—a conclusion, incidentally, that would be expected upon consideration of the surface free energy, large for Ti (2.570 J m^{-2}) and small for Al (1.085 J m^{-2} [8]) (arguments based on surface free energies are strictly valid only at equilibrium, which a growth process is not; however, the very slow growth rate employed here may justify a reference to surface free energies, not in order to provide firm conclusions, but only in order to reveal trends); (2) the Ti films are pseudomorphic on the two substrates; and (3) the films do not grow much beyond 5 Å on Al{110}, but can grow as thick as about 25 Å on Al{001}. We now use the measured $I(V)$-data to get quantitative information about the atomic structure of these films by QLEED as described below.

4. Analyses of high-coverage Ti on Al{001}

All intensity calculations were done with a FORTRAN version of the CHANGE program [9] on an IBM RISC/6000 workstation model 37T. The Al and Ti potential were taken from the compilation of Moruzzi, Janak and Williams [10]. The calculations involved six phase shifts and 71 beams up to 300 eV, an inner potential $V_0 = -(10 + 3i)$ eV and a root mean square amplitude of atomic vibrations of $\langle u^2 \rangle^{1/2} = 0.12$ Å. The agreement between calculated and observed $I(V)$-curves was gauged on the basis of three R-factors: R_{VHT} [11], r_{ZJ} [12] and R_P [13], as discussed below.

4.1. QLEED analysis

The thickest Ti film grown on Al{001} in this study (about 25 Å) yields a fairly good LEED pattern that allows collection of reliable intensity data. The film is thick enough to be considered semi-infinite for electrons with energies between 40 and 360 eV as used in the present LEED experiments. Thus the model calculations involve a semi-infinite Ti{001} film with the in-plane lattice constant of Al{001} ($a = 2.8635$ Å) and with bulk and surface interlayer spacings to be determined.

The bulk interlayer spacing for Al{001} is $d_{bulk} = 2.0248$ Å, the theoretical value for the bulk interlayer spacing of fcc Ti is $d_{bulk} = 2.04$ Å [3]. Accordingly, the search for the best-fit parameters was done by varying d_{bulk} from 1.75 to 2.25 Å, in steps of 0.05 Å, in each case varying Δd_{12} (the change with respect to d_{bulk} of the first interlayer spacing d_{12}) from -0.2 to $+0.2$ Å in steps of 0.05 Å. In the refinement stages, the steps were narrowed to 0.03 Å around the optimum values.

Table 1. 25 Å film of Ti on Al{001}: best-fit parameters. Minima of the R-factors R_{VHT} [11], r_{ZJ} [12] and R_P [13] are given for the parameters: d_{bulk} = bulk interlayer spacing; Δd_{12} = change in the first interlayer spacing; Δd_{23} = change in the second interlayer spacing.

R-factors	d_{bulk} (Å)	Δd_{12} (Å)	Δd_{23} (Å)
$R_{VHT} = 0.302$	2.150	-0.15	0
$r_{ZJ} = 0.154$	2.150	-0.15	0
$R_P = 0.337$	2.132	-0.10	0
$r_{ZJ} = 0.156$	2.132	-0.16	$+0.05$
$R_{VHT} = 0.308$	2.132	-0.13	$+0.05$

It is rather common for the three R-factors listed above to exhibit minima at somewhat different values of the structural parameters, and this is the case in the present study as well.

In addition, we find that R_{VHT} and r_{ZJ} exhibit *two* minima at slightly different parameter values. Table 1 summarizes the results.

The $I(V)$-curves calculated with any one of the parameter sets listed in table 1 are practically indistinguishable from one another on the basis of visual inspection. We therefore quote the final results as the averages of the data in table 1 as follows:

$$d_{bulk} = 2.14 \pm 0.03 \text{ Å} \qquad \Delta d_{12} = -0.14 \pm 0.05 \text{ Å} \qquad \Delta d_{23} = 0.0 \pm 0.05 \text{ Å}.$$

The $I(V)$-spectra calculated with these average parameters are plotted in figure 1 together with two sets of experimental data. The dotted curves are the 'normal' data obtained by normalization to constant incident current and by background subtraction from the raw experimental data; the solid curves have in addition been L-corrected (i.e., corrected for the position-dependent transparency of the LEED-optics grids, see [14]). Despite some obvious blemishes, we consider the overall agreement in figure 1 rather satisfactory.

The conclusion is therefore that the Ti film, pseudomorphic to the Al{001} substrate, has a body-centred tetragonal structure, presumably as a result of the epitaxial strain imposed by the pseudomorphism. To find what the equilibrium (i.e., the unstrained) phase of the film grown is we must do a strain analysis.

4.2. Strain analysis

We first attempt to do a strain analysis for the 25 Å Ti film on Al{001} by comparing the experimental strain ratio to the theoretical strain ratio (see, e.g., [15]) and by assuming that the equilibrium phase is the fcc modification of Ti. The (theoretical) lattice constant of fcc Ti is $a_0^{eq} = 4.08$ Å [3], and hence $d_{bulk}^{eq} = 2.04$ Å. The experimental values measured on the Ti film are: $a_0^{film} = 4.05$ Å (the in-plane lattice constant, equal to that of Al{001}) and $d_{bulk}^{film} = 2.14$ Å. Hence the in-plane strain is

$$\epsilon_1 = \frac{a_0^{film} - a_0^{eq}}{a_0^{eq}} = -0.0074 \tag{2}$$

while the perpendicular strain is

$$\epsilon_3 = \frac{d_{bulk}^{film} - d_{bulk}^{eq}}{d_{bulk}^{eq}} = +0.049 \tag{3}$$

and so the experimental strain ratio r_s^{exp} is

$$r_s^{exp} = \frac{\epsilon_3}{\epsilon_1} = -6.62. \tag{4}$$

The theoretical strain ratio r_s^{th} for a film on a cubic {001} surface is [15]

$$r_s^{th} = -\frac{2c_{12}}{c_{11}} = -\frac{2\nu}{1 - \nu} \tag{5}$$

and therefore can be calculated if one knows the elastic constants c_{11} and c_{12} or the Poisson ratio ν of the equilibrium phase, which in the present case must be either fcc Ti or bcc Ti. The elastic constants for either phase are not known experimentally, but for fcc Ti an estimate can be obtained from theory.

Kraft *et al* [16] have derived a formula relating the strain-energy density around a cubic structure of volume V_0 per atom ($\delta E / V_0$) to the strains expressed in terms of $\delta(c/a)/(c/a)$
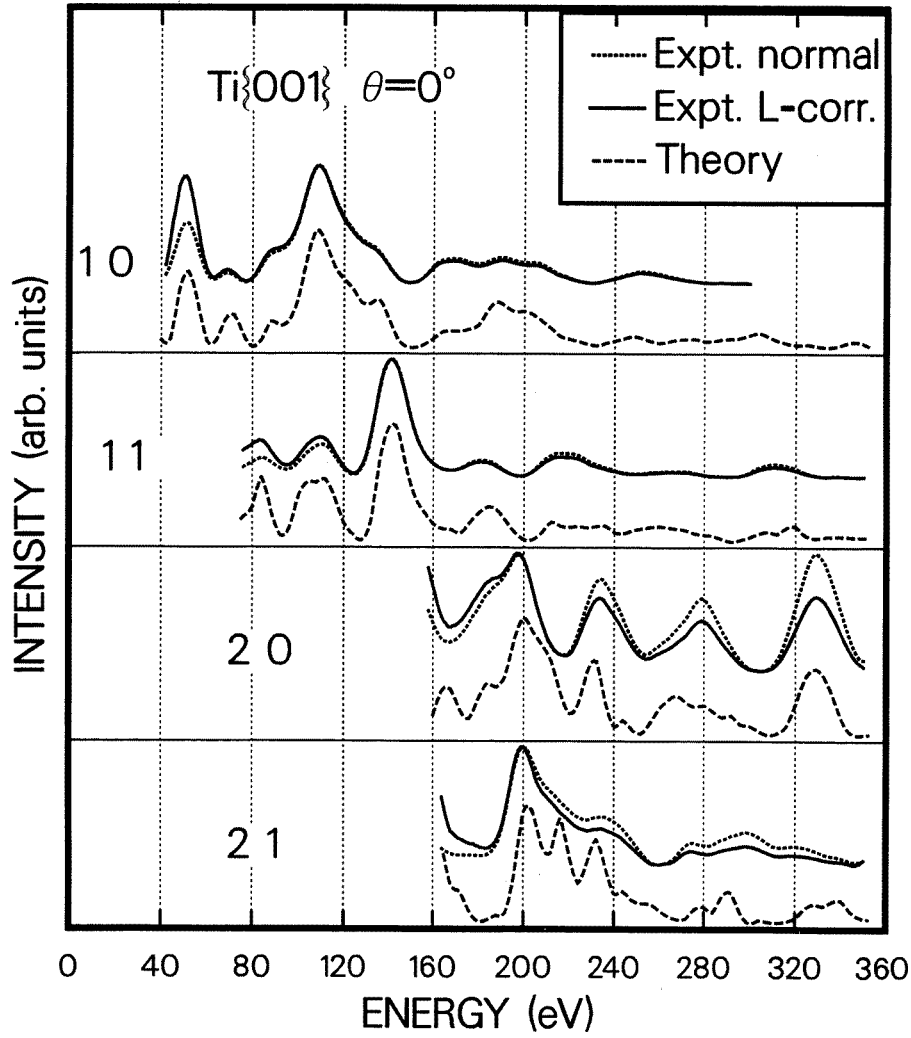
Figure 1. Experimental $I(V)$-spectra for a 25 Å Ti film on Al{001} (dotted and solid lines—see the text for the difference) compared to theoretical $I(V)$-spectra (dashed lines) calculated for a semi-infinite Ti crystal pseudomorphic with Al{001} with the parameters given in the text.

and $\delta V / V$ (c and a are the lattice constants of tetragonal phases, which include the bcc phase for $c/a = 1$ and the fcc phase for $c/a = \sqrt{2}$). At constant volume V the formula is

$$\frac{\delta E}{V_0} = \frac{2}{3} G \left(\frac{\delta (c/a)}{c/a} \right)^2 \tag{6}$$

where G is the shear modulus $G = (c_{11} - c_{12})/2$. The strain-energy density for Ti as a function of c/a at constant V has been calculated by Craievich *et al* [17], and their curve can be used to estimate the shear modulus G from equation (6). The result is $G = 0.2$ Mbar.

Combining this value of G with the calculated [18] value of the bulk modulus $B = 1.09$ Mbar ($B = (c_{11} + 2c_{12})/3$) for fcc Ti, we find $c_{11} = 1.34$ Mbar and $c_{12} = 0.94$ Mbar, and hence $\nu = c_{12}/(c_{11} + c_{12}) = 0.41$. (For comparison, the experimental values for hcp Ti

range for c_{11} from 1.23 to 1.76 Mbar and for c_{12} from 0.996 to 0.869 Mbar [19].) We are therefore in a position to estimate the theoretical strain ratio r_s^{th}: we find it to be equal to -1.4—rather different from r_s^{exp}—which suggests that fcc Ti is not the equilibrium phase.
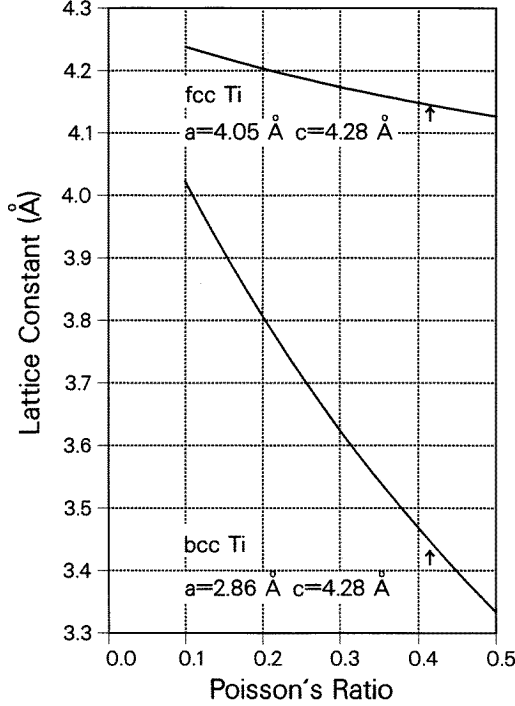

Figure 2. A graph of equation (7), i.e., the lattice constant of the equilibrium phase versus Poisson's ratio for fcc Ti (top) and bcc Ti (bottom). The data for a and c are the data measured on the 25 Å Ti film; the arrows are drawn at the value 0.41 of the Poisson ratio (see the text).

However, before giving up on fcc Ti, we note that the experimental strain ratio for fcc Ti is calculated by using a *theoretical* value of the lattice constant, and such theoretical values are known to be underestimates by 1 to 2% for the 3d non-magnetic transition elements [3]. We therefore invert the problem, assume that the value of ν is known and find the lattice constant from the experimental strain. We use the expression that relates the lattice constant a_0^{eq} of the equilibrium phase to the experimental values of the in-plane and perpendicular lattice constants of the film, a_0^{film} and c^{film}, respectively, [15]:

$$a_0^{eq} = \frac{2\nu}{1+\nu} a_0^{film} + \frac{1-\nu}{1+\nu} c^{film} \tag{7}$$

and we plot the right-hand side of equation (7) for several values of ν from 0.1 to 0.5 in figure 2 for both fcc and bcc Ti.

It is obvious from the figure that the theoretical value $a_0^{eq} = 4.08$ Å for fcc Ti does not cross the curve of equation (7) at physically acceptable values of the Poisson ratio—a confirmation of the disagreement between r_s^{exp} and r_s^{th} found above. The same can be said for bcc Ti, for which $a_0^{eq} = 3.31$ Å at 900 °C and hence about 3.28 Å at room temperature.

However, we can use the value 0.41 for the Poisson ratio to determine the equilibrium lattice constants. From figure 2 (arrows at $\nu = 0.41$) we see that for fcc Ti, $a_0^{eq} = 4.146$ Å and for bcc Ti, $a_0^{eq} = 3.455$ Å. We can therefore immediately eliminate bcc Ti from

consideration as the equilibrium phase, not only because the value 3.455 Å is quite different from the experimental value 3.28 Å, but also because the in-plane strain would be -17.2% and the perpendicular strain $+23.9\%$, both much too large to allow growth of 25 Å films. However, the value 4.146 Å for the lattice constant of unstrained fcc Ti is reasonable. It is only about 1.5% larger than the theoretical value 4.08 Å, and the associated strains are acceptable: 2.3% in-plane and 3.2% perpendicular.

We note that this estimate of the fcc Ti lattice constant is confirmed by the very plausible argument given in [1] for the same purpose, namely, that the near-neighbour distance in the close-packed planes of hcp Ti should be the same in fcc Ti. This argument works well in comparing hcp and fcc Co, where bulk lattice constants have been measured, and yields the fcc Ti lattice constant as 4.17 Å, close to the 4.15 Å found above, and significantly greater than the value from first-principles theory. We conclude that the Ti films that we have grown on Al{001} had a strained fcc structure in epitaxial compression.

5. Results for low-coverage Ti on Al{110} and Al{001}

We now report results of the study of low-coverage films of Ti on Al{110} and Al{001}. On Al{110} the QLEED analysis gives a moderate fit to experiment that determines the principal structural parameter, the distance of a pseudomorphic Ti overlayer from the Al substrate. On Al{001} we report the existence of a c(2×2) phase, but fail to find any structural parameters. Since we are applying in both cases well-tested techniques with which we have long experience, we believe that this partial information is reliable and useful for future studies of these systems.

5.1. Ti on Al{110}

As described in section 3, the LEED pattern of the clean substrate surface worsens rapidly with increasing surface coverage by Ti. The large background makes it increasingly difficult to collect reliable intensity data. For this reason we did not attempt any quantitative analysis of the high-coverage patterns—we limited ourselves to attempting an analysis of the low-coverage pattern, i.e., the one from a 2 Å film. Although we were aware of the fact that this film was very probably not wholly continuous, and certainly not flat, we hoped that it would involve *mostly* only one layer and we thought that it may be possible to determine its structure quantitatively.

We tried a few different models. The simplest involves a single flat layer of Ti pseudomorphic to the Al{110} substrate with the Ti atoms located in the positions that would be occupied by Al atoms if the substrate grew; the interlayer distance was varied by 0.25 Å on either side of the Al{110} interlayer spacing of 1.43 Å. It turns out that this model gives the best agreement with experiment among the models tested, which were: a compositionally disordered Ti–Al alloy in the first atomic layer; a single Ti layer over a Ti–Al alloy in the second layer; a 100% Al first layer and a 100% Ti second layer.

Even the 'best' model—a Ti overlayer 1.58 Å above the Al substrate (i.e, with a 0.15 Å larger interlayer distance than in pure Al{110}) with the first Al–Al interlayer spacing contracted by 0.1 Å—does not provide a good fit to experiment: the R-factors are $R_{VHT} = 0.37$, $r_{ZJ} = 0.25$, $R_P = 0.51$. But considering the fact that the film very probably involved a few regions with different 1×1 structures (i.e., regions with one Ti layer, regions with two Ti layers, bare substrate regions, etc, all of which affect the $I(V)$-curves), we are satisfied that the model is good enough to give some structure information. The fit can be gauged visually for seven beams in figure 3 and shows a correspondence that
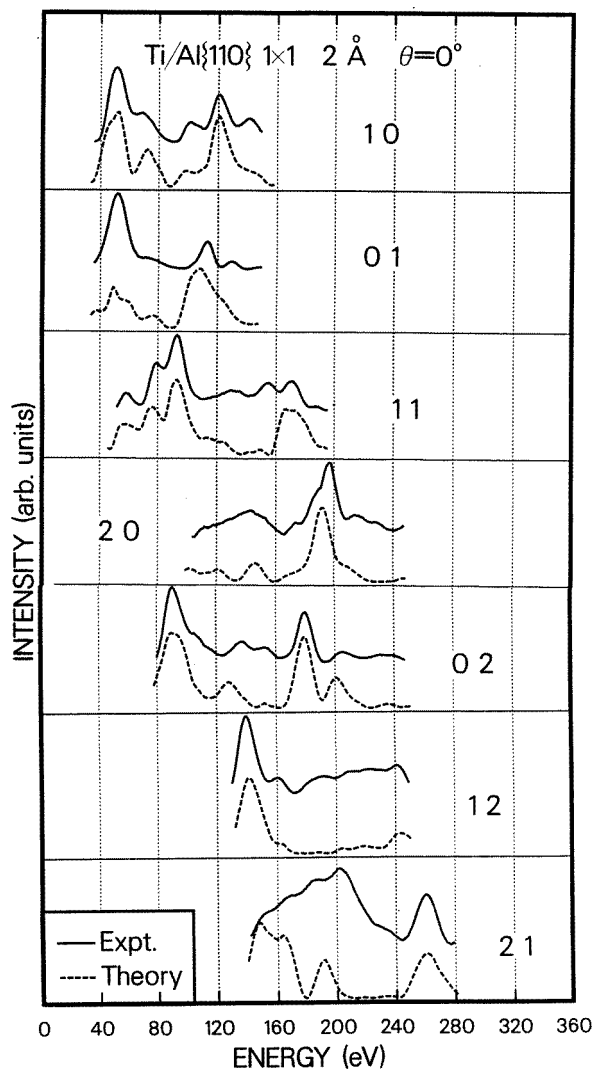
Figure 3. Experimental $I(V)$-spectra from a 2 Å Ti film on Al{110} (solid lines) compared to theoretical $I(V)$-spectra calculated for a pseudomorphic monolayer of Ti on Al{110} (dashed lines).

we judge from experience to be adequate for the determination of the principal structure parameter, although the experimental error is estimated to be ±0.1 Å.

5.2. Ti on Al{001}: low coverage

We mentioned in section 3 that at low surface coverages the LEED pattern exhibits the fractional-order beams characteristic of a c(2×2) structure. These beams are broad and not very intense (whereas the integral-order beams remain almost as sharp as in the pattern of the clean surface); they increase slightly in intensity with increasing coverage, but then fade out and are undetectable when the surface coverage reaches about 7 to 10 Å.

These observations suggest that the c(2×2) structure is limited to relatively small regions of the surface which then grow somewhat larger, but are rather quickly covered by more Ti atoms before they can grow large and produce sharp LEED beams. We collected intensity data from the $\frac{1}{2}\frac{1}{2}$ and the $\frac{1}{2}\frac{3}{2}$ beams from a film of about 4.4 Å: the beams were broad, as mentioned above, and the LEED pattern had a rather high background. We tried to fit the experimental data with different models involving c(2×2) overlayers and/or mixed layers. We disregarded the integral-order spectra, since we suspected that they probably had unknown contributions from regions with different 1×1 structures. We found no model that can be called a solution of the problem. The only model that produced fair agreement with the $\frac{1}{2}\frac{3}{2}$ spectrum (but poor agreement with the $\frac{1}{2}\frac{1}{2}$ spectrum) is an ordered, mixed Ti–Al, slightly buckled *under*layer. Thus, in this model, the Ti atoms reside in the *second* layer on a c(2×2) net with Al atoms. But a definite assignment would require more experimental data from a better developed and more widely extended c(2×2) structure.

6. Conclusion

The 1×1 structure of Ti on Al{001} is well understood. Our QLEED analysis finds it to be body-centred tetragonal with an in-plane lattice constant of $4.05/\sqrt{2} = 2.864$ Å, and with a perpendicular lattice constant of $2.14 \times 2 = 4.28$ Å. Our strain analysis finds that this structure cannot be strained bcc, but is indeed strained fcc. Thus, the most significant result of the present work is that it proves the existence of an epitaxially stabilized fcc phase of Ti, and it determines the lattice constant of this phase to be 4.146 ± 0.025 Å (the error bars result from the experimental error in the determination of the bulk interlayer spacing d_{bulk}, but do not take into account the uncertainty in the value of the Poisson ratio).

The present work provides a good opportunity to point out the value of a strain analysis combined with results of a LEED structure analysis. We note that QLEED just gives us the tetragonal structure of the strained film. Some type of strain analysis is essential to decide if this structure is strained bcc or a strained fcc, or even strained hcp (produced by an anisotropic in-plane epitaxial strain).

The strain analysis can provide both negative and positive arguments about a structure. Thus the curve in figure 2 of possible equilibrium lattice constants of bcc Ti (a_0 versus Poisson ratio ν) combined with the experimentally known value $a_0^{eq} = 3.28$ Å provides an absolute negative argument that rules out the bcc structure. This argument does not require knowledge of the Poisson ratio of bcc Ti, since the curve in figure 2 shows that no acceptable value of the Poisson ratio exists at the known value of a_0^{eq}. The exclusion of the bcc structure is reinforced by the arguments in section 4, namely that assuming the Poisson ratio of bcc Ti to be the same as that of fcc Ti (the theoretical bulk moduli [3] are 1.045 Mbar for bcc Ti and 1.090 Mbar for fcc Ti) one finds a value of a_0^{eq} which is very different from the measured value, and corresponds to a very large strain on the Al{001} surface.

Conversely, strain analysis provides a positive argument for the fcc structure. The LEED data, which give the curve in figure 2, combined with the theoretical estimate of ν, yield a value of a_0^{eq} for fcc Ti that is only 1.5% larger than the theoretical fcc Ti lattice constant. Moreover, the theoretical values based on the local-density approximation are known to be low for the 3d transition metals by 1 to 2%: the theoretical value of a_0^{eq} for bcc Ti is 3.23 Å, which is 1.5% lower than the experimental value of 3.28 Å. Thus the strain analysis provides a positive argument for the fcc structure, which is reinforced by the moderate strains on Al, and by the qualitative argument that the near-neighbour distance in the close-packed layers should be about the same as in hcp Ti.

Our experiments show that films of Ti grown on Al{110} do not produce useful LEED patterns beyond thicknesses of 5 to 6 Å, corresponding to two to three atomic layers. This is only a small disagreement with the report of SSS, who find the 'critical' thickness to be five layers from high-energy ion-scattering experiments, but only three layers from photoemission [1]. (Recall that the estimated error in *our* thickness determinations is about ±50%.) We are able to do a partial structure determination of a monolayer of Ti on Al{110} and we thereby confirm the pseudomorphism of the overlayer, but of course one layer is not enough to identify the equilibrium phase.

For films grown on Al{001} we find the occurrence of a poorly developed (weak LEED pattern) c(2×2) structure in the early stages of growth, and then the formation of a well-crystallized 1×1 phase for films thicker than about 10 Å. After completion of our work we became aware of similar experiments [20] on Al{001} (unpublished at the time of writing) in the same group that first reported the Ti/Al{110} results. The results of these experiments differ from ours on two points: (1) the c(2×2) structure was not observed; and (2) the 'critical' thickness of Ti films on Al{001} was found to be about 5.5 layers (which with the interlayer spacing that we have determined here corresponds to about 12 Å). We do not consider the first discrepancy very significant: the non-observation of a c(2×2) structure could be explained by the fact that the workers did not use LEED in their experiments, and hence they could not have seen the c(2×2) structure even if it had been present. The second discrepancy may be more important, particularly because our thickest (25 Å) film might have grown thicker if we had continued the growth, and might still have produced fairly good LEED patterns. We leave this question open for the time being.

In closing, we would like to note the puzzling behaviour of Al surfaces with regard to heteroepitaxy. The work of SSS [1] and the present study clearly show that Al{110} and Al{001} support rather well the growth of epitaxial and pseudomorphic films of Ti (although the behaviour in the very early stages is not clear). By contrast, Al{001} and Al{111} lose their long-range order almost immediately when put in contact with small amounts of Fe [21] or Co (unpublished). Fractions of a monolayer of either Fe or Co react with and displace Al atoms in the whole surface selvedge and as a consequence completely destroy the LEED pattern. These phenomena are not understood at the present time.

Acknowledgments

References

[1] Saleh A A, Shutthanandan V and Smith R J 1994 *Phys. Rev.* B **49** 4908
[2] Pearson W B 1967 *Lattice Spacings and Structures of Metals and Alloys* vol 2 (Oxford: Pergamon)
[3] Moruzzi V L and Marcus P M 1993 *Handbook of Magnetic Materials* vol 7, ed K H J Buschow (New York: North-Holland) ch 2, p 97 *et seq*
[4] Davis L E, MacDonald N C, Palmberg P W, Riach G E and Weber R E 1978 *Handbook of Auger Electron Spectroscopy* (Eden Prairie, MN: Physical Electronics Industries Inc.)
[5] Seah M P and Dench W A 1979 *Surf. Interface Anal.* **1** 2
[6] Jona F, Strozier J A Jr and Marcus P M 1985 *The Structure of Surfaces* ed M A Van Hove and S Y Tong (Berlin: Springer) p 92
[7] Jona G and Marcus P M 1995 *Crit. Rev. Surf. Chem.* at press
[8] Mazey L Z and Giber J 1982 *Japan. J. Appl. Phys.* **21** 1569
[9] Jepsen D W 1980 *Phys. Rev.* B **22** 814, 5701

[10] Moruzzi V L, Janak J F and Williams A R 1978 *Calculated Electronic Properties of Metals* (New York: Pergamon)
[11] Van Hove M A, Tong S Y and Elconin M H 1977 *Surf. Sci.* **64** 85
[12] Zanazzi E and Jona F 1977 *Surf. Sci.* **62** 61
[13] Pendry J B 1980 *J. Phys. C: Solid State Phys.* **13** 937
[14] Kim S K, Jona F and Strozier J A Jr 1995 *Phys. Rev.* B at press
[15] Jona F and Marcus P M 1991 *Surface Physics and Related Topics* ed Fu-Jia Wang, Guang-Jiong Ni, Xun Wang, Kai-Ming Zhang and Dong Lu (Singapore: World Scientific) p 213
[16] Kraft T, Marcus P M, Methfessel M and Scheffler M 1993 *Phys. Rev.* B **48** 5886
[17] Craievich P J, Weinert M, Sanchez J M and Watson R E 1994 *Phys. Rev. Lett.* **72** 3076
[18] Moruzzi V L and Marcus P M 1993 *Phys. Rev.* B **48** 7665
[19] Simmons G and Wang H 1971 *Single Crystal Elastic Constants and Calculated Aggregate Properties: A Handbook* (Cambridge, MA: MIT Press)
[20] Saleh A A 1994 *PhD Thesis* Montana State University
[21] Begley A M, Tian D, Jona F and Marcus P M 1993 *Surf. Sci.* **280** 289